2009 First International Conference on Advances in Satellite and Space Communications

Reduced Cluster Search ML Decoding for QO-STBC Systems

Isaque Suzuki, Taufik Abrão
Dept. of Electrical Engineering
State University of Londrina
86051-990, PR, Brazil
taufik@uel.br

Bruno A. Angélico, Fernando Ciriaco
Paul Jean E. Jeszensky
Dept. of Telecomm. & Control Engineering
Escola Politécnica, University of São Paulo
São Paulo, 05508-900, SP, Brazil
{angelico, fciriaco, pjj}@lcs.poli.usp.br

Fernando Casadevall
Dept. of Signal Theory & Communication
Universitat Politècnica de Catalunya
08034 Barcelona, Spain
ferranc@tsc.upc.edu

***Abstract*—Since the maximum likelihood (ML) decoding results too complex when the modulation order and the number of receive antennas increase, an efficient reduced complexity ML-based decoding scheme applied to a multiple-input-multiple-output (MIMO) antenna systems with quasi-orthogonal space-time block code (QO-STBC) is proposed, and named reduced cluster search ML decoding (RCS-ML). Its performance and complexity aspects are compared to the conventional ML decoding approach. High-order modulation indexes and short low density parity check codes (LDPC) are considered. Numerical results have indicated no degradation in the performance and an increasing reduction in the complexity of RCS-ML decoding with respect to the conventional ML when the modulation order increases.**

***Index Terms*—MIMO system, QO-STBC, ML decoding, cluster search, LDPC.**

I. Introduction

The last five years have been dominated by high demands on video and audio data with reliability real-time applications. Multiple-input-multiple-output (MIMO) schemes, associated with space-time block codes (STBC), for instance, Alamouti rate 1 STBC [1] (R1 STBC), represent a suitable solution and are frequently incorporated by many standards like WiMAX. Furthermore, higher throughput with acceptable performance $\times$ complexity trade-off can be achieved through the inclusion of a bit-mapped coded modulation (BMCM) structure. BMCM in conjunction with parallel short low density parity check codes (LDPC), quasi-orthogonal STBC (QO-STBC) [2], and iterative soft parallel interference cancellation (PIC) detector, is discussed in [3]. The aim is to achieve low complexity schemes, high throughput with good performance and to generate low processing delay in the overall processing of detection and decoding. Good STBC designs must take into account jointly performance criteria coding gain, diversity gain, multiplexing gain, and the decoder complexity.

In this scenario, the so called fast-decodable SBTC MIMO schemes have been considered recently with great interest. Previous works on fast-decodable low-complexity SBTC MIMO systems includes [4]–[9]. In [7], a family of full-rate, full-diversity 2×2 codes, whose detection complexity grows only quadratically with the size of the signal constellation have been proposed. Thus, the optimum decoder complexity reduced by a factor of 256 for the 16-QAM signal constellation (and by $4,096$ for the 64-QAM modulation). A different approach to achieve low-complexity near-maximum likelihood QO-STBC decoding based on iterative interference cancellation (IICIS) was proposed in [6].

In order to fulfill the requirements of system capacity, low power consumption and low terminal size, development of LDPC decoders[1] has been focused by many recent papers. However, the LDPC were introduced since 1962 by Gallager [10], showing the possibility of achieving capacity by coding a message using long codes, resulting in a good trade-off between complexity and performance. At that time there was no way to implement LDPC codes and they remained forgotten until 1999, when Mackay brought them back to scene [11].

This paper proposes a low-complexity and efficient decoding algorithm for QO-STBCs schemes, based on reduced ML cluster search. The RCS-ML decoder performs similarly to the conventional ML in terms of bit error rate (BER), but with lower complexity that is more evident for higher order modulations. Performance results were obtained with and without LDPC codes. The remaining sections are organized as follows: Section II describes the QO-STBC MIMO system with short parallel LDPC inner codes. The proposed reduced cluster search ML decoder in the context of QO-STBC codes is discussed in Section III. Numerical results and complexity analysis for the proposed QO-STBC decoder with an arbitrary number of receive antennas are analysed in Section IV. Main conclusions are presented in Section VI.

II. QO-STBC System Model

A MIMO system with $n_T = 4$ transmit antennas and $n_R \geq 1$ receive antennas is considered, with 4 symbols transmitted simultaneously. Additionally, $n_T n_R$ independent flat fading subchannels, M-QAM modulation, Rate 1 QO-STBC scheme of [2], and short LDPC (optionally) are employed, Fig. 1.

A. LDPC Encoding

In order to achieve high throughput (herein, up to 4 bits per symbol period was considered, depending on the modulation

[1] In many of them, complexity scales linearly with code length.

978-0-7695-3694-1/09 $25.00 © 2009 IEEE
DOI 10.1109/SPACOMM.2009.18

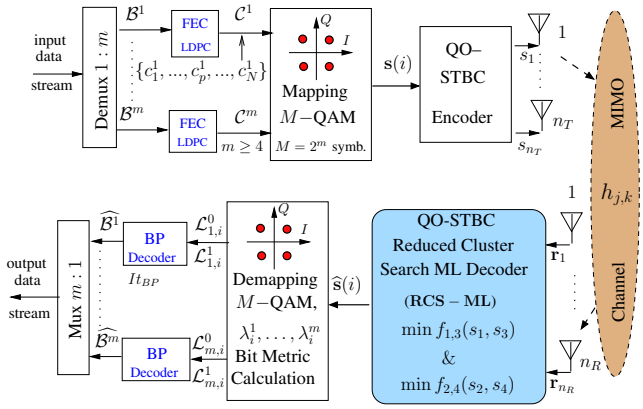

Figure 1. QO-STBC with short LDPC MIMO system and reduced cluster search ML decoding approach (RCS-ML). $n_T = 4$ and $n_R \geq 1$ antennas.

index and coding rate), associated to suitable performance and simplicity of decoding at the receiver, the bit-mapped coded modulation (BMCM) scheme is used, jointly with m short parallel LDPC coding [12]. The adopted modulation is high-order squared-QAM modulation and $m = 2, 4, 6$ or 8.

Initially, as shown in Fig. 1, the input data stream is demultiplexed into m data substreams $\{\mathcal{B}^i\}_{i=1}^m$ with block lengths K_i. To keep the decoding complexity low, each substream $\mathcal{B}^i$ is encoded using a LDPC code, obtaining m codewords $\mathcal{C}^i$, i.e., $\{\mathcal{C}^i\}_{i=1}^m$, of length N; the pth encoded bit in $\mathcal{C}^i$ is denoted c_p^i. Observe that there is an inherent flexibility in the BMCM structure: substreams can be encoded using LDPC codes with different values of K_i, as long as all m codes produce codewords of the same length N. Hence, the overall rate of the m LDPC codes is given by

$$R_{\text{ldpc}} = \frac{\sum_i^m K_i}{mN}. \tag{1}$$

Assuming identical block lengths, $K_i = K$, the overall rate of the m LDPC(N, K) codes is simplified to: $R_{\text{ldpc}} = \frac{K}{N}$.

All the m LDPC encoding processes are simply done in parallel. The ith LDPC encoding process is given by $\mathcal{C}^i = \mathcal{B}^i\mathcal{G}^i$, where $\mathcal{G}^i$ is the $K_i \times N$ generator matrix of the ith LDPC code component.

B. R1 QO-STBC

The pth bits from all m LDPC codewords simultaneously select the pth 2^m-ary constellation point $s_i \in \mathcal{S}$, where $\mathcal{S}$ is a set of all valid symbols belonging to the adopted constellation at the transmitter.

The topology of Fig. 1 employs rate 1 quasi-orthogonal space-time block code (R1 QO-STBC) proposed in [13], described by the code matrix

$$\mathcal{A} = \begin{pmatrix} s_1 & s_2 & s_3 & s_4 \\ -s_2^* & s_1^* & -s_4^* & s_3^* \\ -s_3^* & -s_4^* & s_1^* & s_2^* \\ s_4 & -s_3 & -s_2 & s_1 \end{pmatrix}. \tag{2}$$

Four new constellation points (s_1, s_2, s_3, s_4) are transmitted using $n_T = 4$ and $L = 4$ time slots, such that

$$R_{\text{stbc}} = \frac{\#\text{symbols transmitted}}{\#\text{time slots used}, L} = 1 \quad \text{(Rate 1)}, \tag{3}$$

and the overall throughput for a system using a M-ary constellation is defined as

$$\Theta = R_{\text{stbc}} R_{\text{ldpc}} \log_2 M \qquad \text{[bits per symbol period]}. \tag{4}$$

C. Receiver

Let $x(i)$ be the ith modulated symbol with duration T_s, and $s_j(t)$ the transmitted symbol by the jth transmit antenna at time t. Each transmitted symbol goes through the wireless channel to arrive at each of n_R receive antennas. Denoting the path gain from transmit antenna j to receive antenna k at each symbol interval by $h_{kj}(t)$, the baseband discrete-time signal received at the kth antenna is given by

$$r_k(t) = \sum_{j=1}^{n_T} h_{kj}(t) s_j(t) + n_k(t), \qquad t = 1, ..., L, \tag{5}$$

where $h_{kj}(t), \forall k \in \{1, 2, \ldots, n_R\}, \forall j \in \{1, 2, \ldots, n_T\}$ are assumed to be i.i.d. complex Gaussian random variables (fading amplitudes are Rayleigh distributed) with zero mean and $\mathbb{E}[(h_{kj}^I)^2] = \mathbb{E}[(h_{kj}^Q)^2] = \frac{1}{2}$, where h_{kj}^I and h_{kj}^Q are the real and imaginary parts of $h_{kj}(t)$. The complex additive white Gaussian noise (AWGN) at the kth receive antenna, $\{n_k\}, k = 1, \ldots, n_R$, has zero mean and variance

$$\mathbb{E}[n_k^2] = N_0 = \frac{n_T \overline{E}_s}{\gamma} = \frac{n_T \overline{E}_s}{m 10^{\frac{\text{SNR}}{10}} R_{\text{stbc}} R_{\text{ldpc}}}, \tag{6}$$

where $\overline{E}_s$ is the average energy of the transmitted symbols, given a constellation format, SNR is the signal-to-noise ratio per receive antenna in decibels (dB), and γ is the average SNR per receive antenna [2].

The received signals from all receive antennas can be rearranged in a vectorial form, such that

$$\mathbf{r}(t) = \mathbf{H}(t)\mathbf{s}(t) + \mathbf{n}(t), \qquad t = 1, ..., L, \tag{7}$$

where, in each time slot $t = 1, ..., 4$ of the adopted QO-STBC scheme, $\mathbf{r}(t) = [r_1(t)\, r_2(t)\, \ldots\, r_{n_R}(t)]^T$ is the received signal vector, $\mathbf{s}(t) = [s_1(t)\, s_2(t)\, \ldots\, s_{n_T}(t)]^T$ is the transmitted symbol vector, $\mathbf{H}(t)$ is the $n_R \times n_T$ channel matrix with channel coefficients $\{h_{kj}\}_{k,j=1}^{n_T,n_R}$ between the jth transmitted antenna and kth receive antenna, and $\mathbf{n}(t) = [n_1(t)\, n_2(t)\, \ldots\, n_{n_R}(t)]^T$ is the sampled noise vector. The channel matrix coefficients are assumed to be perfectly known at the receiver, but completely unknown at the transmitter.

D. ML Decoding

The maximum likelihood decision metric is obtained by minimizing the two sum terms [13]

$$(\widehat{s}_1, \widehat{s}_2, \widehat{s}_3, \widehat{s}_4) = \tag{8}$$
$$\arg \min_{s_1, s_4 \in \mathcal{S}} f_{1,4}(s_1, s_4), \quad \arg \min_{s_2, s_3 \in \mathcal{S}} f_{2,3}(s_2, s_3),$$

$$f_{1,4}(s_1,s_4)=\sum_{k=1}^{n_R}\left[\left(\sum_{j=1}^{n_T=4}|h_{jk}|^2\right)\left(|s_1|^2+|s_4|^2\right)+2\Re\left\{(-h_{1k}r_k^*(1)-h_{2k}^*r_k(2)-h_{3k}^*r_k(3)-h_{4k}r_k^*(4))s_1\right.\right.$$
$$\left.\left.+\ (-h_{4k}r_k^*(1)+h_{3k}^*r_k(2)+h_{2k}^*r_k(3)-h_{1k}r_k^*(4))\,s_4+(h_{1k}h_{4k}^*-h_{2k}^*h_{3k}-h_{2k}h_{3k}^*+h_{1k}^*h_{4k})s_1s_4^*\right\}\right] \quad (9)$$

$$f_{2,3}(s_2,s_3)=\sum_{k=1}^{n_R}\left[\left(\sum_{j=1}^{n_T=4}|h_{jk}|^2\right)\left(|s_2|^2+|s_3|^2\right)+2\Re\left\{(-h_{2k}r_k^*(1)+h_{1k}^*r_k(2)-h_{4k}^*r_k(3)+h_{3k}r_k^*(4))s_2\right.\right.$$
$$\left.\left.+\ (-h_{3k}r_k^*(1)-h_{4k}^*r_k(2)+h_{1k}^*r_k(3)-h_{2k}r_k^*(4))s_3+(h_{2k}h_{3k}^*-h_{1k}^*h_{4k}-h_{1k}h_{4k}^*+h_{2k}^*h_{3k})s_2s_3^*\right\}\right] \quad (10)$$

where the cost function to be independently minimized are given by (9) and (10), at the top of the page.

So, for MIMO system with small constellation size, it is computationally viable to evaluate, independently, all possible values for the pairs (s_1, s_4) and (s_2, s_3), using the two cost functions (9) and (10), obtaining directly the ML estimates. However, once the computation complexity increases exponentially with m, it is computationally inefficient to evaluate all pair combinations when the dimension of the constellation is high, for instance $M \geq 16$. Section III describes an alternative low complexity procedure to compute (9) and (10), suitable for high squared-order modulation MIMO QO-STBC with $n_T = 4$ and $n_R \geq 1$.

E. Bit Metric and Belief Propagation Decoders

The last block in the decoding process is performed by low complexity m short parallel LDPC decoders. Herein, the LDPC decoders use *belief propagation* (BP) decoding algorithm, with a maximum number of iterations It_{BP}.

As BP decoders require soft symbol estimates $\mathcal{L}^0_{\mathfrak{m},i}, \mathcal{L}^1_{\mathfrak{m},i}$, and admitting identical noise variance in all n_T receive antennas $\mathbb{E}[n_k^2] = \sigma^2,\ k = 1, \ldots, n_T$, the bit metrics are calculated as:

$$\mathcal{L}^0_{\mathfrak{m},i} = \frac{1}{1+e^{-\lambda_i^{\mathfrak{m}}}}, \qquad \mathfrak{m} = 1, \ldots, m, \quad (11)$$

with $\mathcal{L}^1_{\mathfrak{m},i} = 1 - \mathcal{L}^0_{\mathfrak{m},i}$, and

$$\lambda_i^{\mathfrak{m}} = \frac{1}{2\sigma^2}\left(\min_{\mathfrak{s}\in S_i^{\mathfrak{m},(0)}}\|\widehat{\mathbf{s}}_i-\kappa\mathfrak{s}\|^2-\min_{\mathfrak{p}\in S_i^{\mathfrak{m},(1)}}\|\widehat{\mathbf{s}}_i-\kappa\mathfrak{p}\|^2\right), \quad (12)$$

where κ takes into account path loss and shadowing effects, and the channel coefficients associated to $\mathbf{s}_i$ in (9) or (10) as well; $S_i^{\mathfrak{m},(0)}$ is the set of all constellation points with a zero at i-th position and $S_i^{\mathfrak{m},(1)}$ is the set of all constellation points with one at i-th position. In fact, the soft estimates symbols can be interpreted as

$$\widehat{\mathbf{s}}_i = \kappa\mathbf{s}_i + \eta_i, \quad (13)$$

where η_i is the sum of receiver noise plus interference terms in (9) or (10).

The soft symbol estimates $\mathcal{L}^0_{\mathfrak{m},i}$ and $\mathcal{L}^1_{\mathfrak{m},i}$ are used by BP decoders to compute the log-likelihood ratios (LLRs) passed from variable nodes to check nodes. LLRs are used instead of probabilities because of their higher numerical stability [14]. Hence, BP decoders [12] in Fig. 1 consist of an iterative algorithm that passes messages (LLR values) between variable nodes and check nodes. Computation of (12) is performed recursively until the BP iteration process finishes.

If the matrix of parity checks is satisfied or the algorithm reaches the maximum number of iterations, a hard decision is performed, where positive values of LLRs are considered bit one and negative values are bit zero. After all, each LDPC decoder outputs $\hat{\mathcal{B}}^{\mathfrak{m}}$.

III. Reduced Cluster Search ML Decoding (RCS-ML)

The idea of cluster search came up from observing the cost function behavior, Eqs. (9) and (10), for all possible symbol combinations. As can be seen from the illustrative example in Fig. 2, there is a pattern that repeats itself. This figure was generated considering 16-QAM modulation, resulting in 16 4×4 clusters.

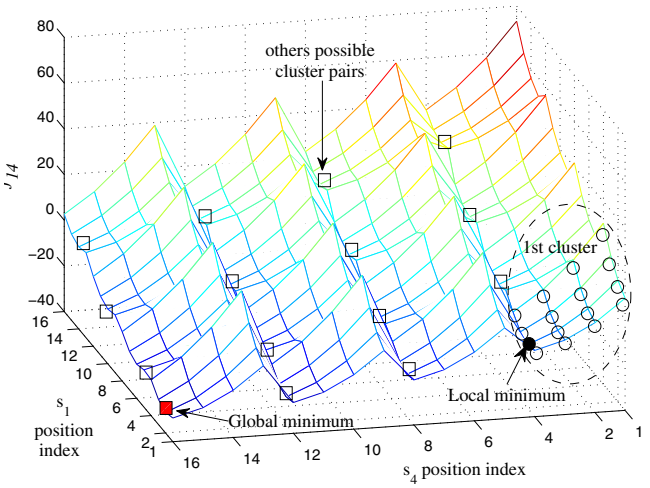

Figure 2. Typical f_{14} values, considering (s_1, s_4) mapping symbol pairs in a 16-QAM modulation as described in Fig. 4.a) and 4.b); circles indicate search values inside the first cluster, and the filled circle is the local minimum. The positions of local minima within the other clusters have the same pattern, regarding the first cluster, as represented by square markers. The same behavior is observed with f_{23} values, considering (s_2, s_3).

This pattern can be described intuitively as follows: given a QAM constellation and a received symbol corrupted by noise, firstly, from constellation mapping in Fig. 3, it could be considered the symbols belonging to one column (or row);

these columns (rows) identifying cluster regions. For 16-QAM, four symbols of first column (i.e., first cluster, constituted by symbols index 1, 2, 3, and 4) are considered. In terms of Euclidean distance from received symbol to the constellation column (row) symbols, two cases can be distinguished:

a) received symbol is closer to the symbol located at the extremities of the selected constellation column (row); in the Fig. 3, this situation is identified by hypothetical received symbols $\triangle$ and $\diamondsuit$, located on cluster-regions I and III, respectively.
b) received symbol is located closer to one or two (if half-way situation) internal symbols of the same column (row) in the constellation; in this example, the received symbol $*$.

In case of hypothesis a) occurs, and if the 1, 2, 3 and 4-th symbol constellation distances computation order is assumed, a monotonic decreasing (received symbols into Region I) or increasing (Region III) pattern for cost functions $f_{1,4}$ or $f_{2,3}$ values is observed. On the other hand, in case of hypothesis b) take place, a parabolic pattern with upwards concavity appears on the $f_{1,4}$ or $f_{2,3}$ evaluations. Besides, this behavior repeats if we consider other columns (or clusters) of the constellation, as can be inferred from Fig. 2. This figure explains the case of cost function be employed to evaluate the distance of a pair of symbols, s_1 and s_4 (or alternatively s_2 and s_3), instead of only one symbol evaluation in eq. (9), say s_1, holding s_4 fixed. Hence, the monotonic (de)creasing or parabolic patterns become 3D surfaces.

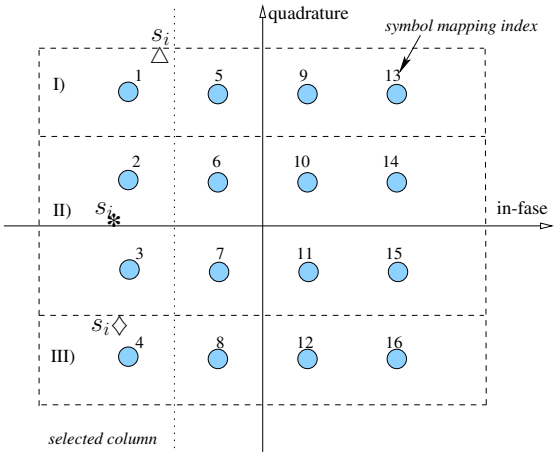

Figure 3. 16-QAM Euclidean distance evaluation by clusters. Two situation can be identified: external and internal received symbol s_i, $i = 1, \ldots, 4$, location regards the selected constellation column symbols.

In summary, the basic idea is to perform a ML search only inside one cluster (for instance, in Figure 2 the first cluster was chosen) in order to find a local minimum, and to generate a sub-set of symbol pairs from the other cluster (other 15 clusters in the 16-QAM example) with the same relative position regarding the local minimum primarily found in the first cluster, resulting in a set of local minima (square markers in Figure 2). The pattern observed in Figure 2 repeats itself at each $\sqrt{2^m}$ symbols for symbol pairs (s_1, s_4) (alternatively (s_2, s_3)), and all pairs inside this pattern constitute a cluster. Finally, the ML search is performed over the generated set of local minima in order to find the global minimum of (9) (or alternatively (10)). Figure 2 shows $f_{1,4}$ values, obtained via cluster search procedure, with global minimum occurrence at ($s_1 = \underline{2}$, $s_4 = \underline{16}$) indexes, square bold marker.

In order to implement the RCS-ML QO-STBC decoding, three steps are carried out considering each of 2^m clusters as indicated in Algorithm 1.

Algorithm 1 RCS-ML QO-STBC

Input: r, H **Output:** $\widehat{s}_1, \widehat{s}_2, \widehat{s}_3, \widehat{s}_4$

step 1: Perform a ML search decoding inside of the first cluster over (s_1, s_4) and (s_2, s_3) symbol pairs, Eqs. (9) and (10);
Symbols of M-QAM constellation are hypothetically mapping as $s_1, s_2, s_3, s_4 \in \{\underline{1}, \underline{2}, \cdots, \underline{\sqrt{2^m}}\}$.

step 2: Record the two pairs $(\check{s}_1, \check{s}_4)$ and $(\check{s}_2, \check{s}_3)$ that locally minimize Eqs. (9) and (10), respectively.

step 3: Generate sets

$$\mathcal{S}_i^{\text{clst}} = \{\underline{\check{s}_i + k\sqrt{2^m}} \mid k = 0, \ldots, \sqrt{2^m} - 1\}, \quad i = 1, \ldots, 4;$$

Perform decoding through all possible cluster pairs (s_1, s_4) and (s_2, s_3), where $s_i \in \mathcal{S}_i^{\text{clst}}$:

$$(\widehat{s}_1, \widehat{s}_4) = \arg \min_{\substack{s_1 \in \mathcal{S}_1^{\text{clst}}; \\ s_4 \in \mathcal{S}_4^{\text{clst}}}} f_{1,4}(s_1, s_4), \quad \text{and}$$

$$(\widehat{s}_2, \widehat{s}_3) = \arg \min_{\substack{s_2 \in \mathcal{S}_2^{\text{clst}}; \\ s_3 \in \mathcal{S}_3^{\text{clst}}}} f_{2,3}(s_2, s_3)$$

In order to illustrate the steps of the Algorithm RCS-ML, consider the clustered 16-QAM QO-STBC decoding sketched in Figure 4. Since the clusters pattern is similar for (s_1, s_4) and (s_2, s_3) pairs, only the cluster search for the (s_1, s_4) pair is described. Initially (step 1), the first column of symbols in Figure 4.a is chosen as a cluster to be evaluated; this set generates all symbol pairs in the white shading cluster of Figure 4.d, used in computation of $f_{1,4}$, and is called $\mathcal{S}_i^{\text{clst}_1} = \{\underline{1}, \underline{2}, \underline{3}, \underline{4}\}$. The dark (red) block into white shading cluster of Figure 4.d, ($s_1 = \underline{2}$, $s_4 = \underline{4}$), indicates the selected pair indexes that yields the minimum value of $f_{1,4}$ inside step 2 (local minimum). The cluster-sets for (s_1, s_4) symbol pair, labelled $\left\{\mathcal{S}_1^{\text{clst}_\mathfrak{m}}, \mathcal{S}_4^{\text{clst}_\mathfrak{m}}\right\}$, $\mathfrak{m} = 1, \ldots, m$, are obtained by selecting $(\check{s}_1)$-th and $(\check{s}_4)$-th row of constellation mapping in Figure 4.a and 4.b, respectively. The resulting symbol pair set (s_1, s_4) calculated inside step 3 is shown in Figure 4.c. After all, the ML search is performed over all pairs generated by the symbol set of Figure 4.c, i.e., in this hypothetical example, $\mathcal{S}_1^{\text{clst}} = \{\underline{2}, \underline{6}, \underline{10}, \underline{14}\}$ and $\mathcal{S}_4^{\text{clst}} = \{\underline{4}, \underline{8}, \underline{12}, \underline{16}\}$. The estimated symbol pair $(\widehat{s}_1, \widehat{s}_4)$ will be that which produces the minimum $f_{1,4}$ value.

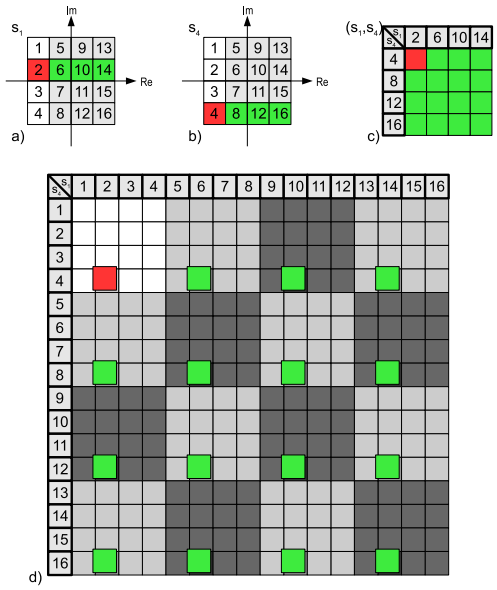

Figure 4. Clusters mapping employed in RCS-ML procedure, considering 16-QAM: hypothetical cluster search for a) symbol s_1; b) symbol s_4; c) symbol pair (s_1, s_4), and d) all clusters mapping for symbol pair (s_1, s_4).

IV. Numerical Results

The main system and channel parameters used in Monte-Carlo simulations are summarized in Table I. In all numerical results shown here, QO-STBC and $M-QAM$ modulation were adopted; in the cases of source coding, short LDPC(204,102) was adopted. For simplicity, it is assumed perfect knowledge of channel state information (CSI) at the receiver side.

In accordance with the most common channel model in the literature [1], [13], herein a quasi-static time-varying channel model is adopted: the fading coefficients remain fixed during each QO-STBC block of $L = 4$ time slots (the quasi-static fading condition is satisfied: $L \cdot T_s < (\Delta t)_c$, the channel coherence time), and vary independently from one block to the next.

Fig. 5 describes the performance of ML and RCS-ML decoding, both in the absence of LDPC coding, for the case of QO-STBC MIMO system with $n_T = 4 \times n_R = 1$ antennas. Besides, Fig. 6 indicates the behavior of both decoders for the case of short LDPC(204,102) QO-STBC MIMO system with $n_T = 4 \times n_R = 1$ antennas employing the ML against RCS-ML decoding. Finally, Fig. 7 compares the performance of both decoders but considering $n_R = 4$ receive antennas under the same short LDPC and QO-STBC coding. It is worth noting that the difference in system performances with RCS-ML and conventional ML decoding is undistinguished for all SNR and constellation size conditions. Those results indicate that even for undetermined system condition ($n_T > n_R$) the RCS-ML algorithm achieves the same BER performances of the ML with exhaustive search. This is due to the adoption of cluster search strategy, allowing a reduction in space search by the use of clustering approach, but yet performing the ML testing overall clustering pair-candidates.

Table I
MIMO System, RCS-ML decoding and channel parameters.

Parameter	Adopted Values
QO-STBC MIMO System	
# Tx antennas	$n_T = 4$
# Rx antennas	$n_R = 1$ or 4
Modulation format	squared M-QAM: $M = 4$, 16, 64, 256
QO-STBC code	Rate 1, $R_{\text{stbc}} = 1$ [13]
Rx SNR per antenna	$SNR \in [-10; 42]$ dB
Throughput	$\Theta = 1.0$, 2.0, 3.0, or 4.0 [bits/symb. period]
LDPC codes	
Number and size	m short LDPC [12], [15]
Rate	LDPC(204, 102), $\Rightarrow R_{\text{ldpc}} = \frac{1}{2}$
Belief Prop. Decoder	$It_{BP} \leq 20$ iterations
Rayleigh Channel	
sub-channel fading	flat-Rayleigh
channel type	quasi-static (slow), $L = 4$
Channel state info.	perfectly known at Rx
RCS-ML Decoding	
cluster size	$\sqrt{2^m} \times \sqrt{2^m}$

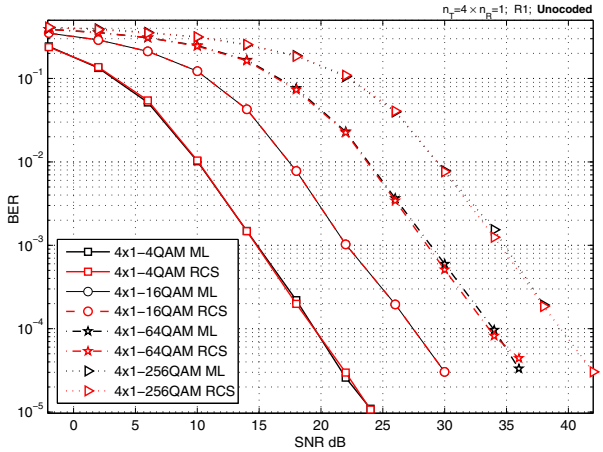

Figure 5. ML against RCS-ML decoding performance comparison for the QO-STBC MIMO system with different QAM constellation size, $n_T = 4 \times n_R = 1$ antennas.

V. Complexity Analysis for the RCS-ML Decoding

In order to evaluate the complexity of the proposed algorithm, real multiplications and sums are considered. Analyzing (9) and (10) and considering each complex multiplication as four real multiplications and each complex sum as two real sums, there are 90 real multiplications and 27 real sums for each f_{14} or f_{23} evaluation. As the proposed algorithm needs only 2^m ML evaluation for step 1 and 2^m for step 2, so, the overall evaluation number is only 2^{m+1}. Table II compares the complexity of RCS-ML QO-STBC and ML QO-STBC decoding schemes. Those complexities can be compared using the perceptual complexity reduction factor, expressed by

$$\text{CR} = \frac{\text{C}_{RCS}}{\text{C}_{ML}} \times 100 \quad = \quad 2^{1-m} \times 100 \quad [\%]. \quad (14)$$

where the second equally holds for all analyzed constellations and number of received antennas.

From Table II one can conclude an increasing reduction in the computational complexity index CR when the modulation

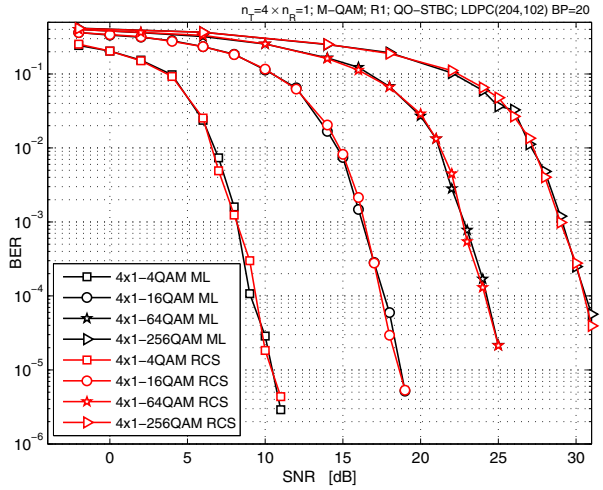

Figure 6. ML against RCS-ML decoding performance comparison for the QO-STBC MIMO system with short LDPC(204,102) and $n_T = 4 \times n_R = 1$ antennas.

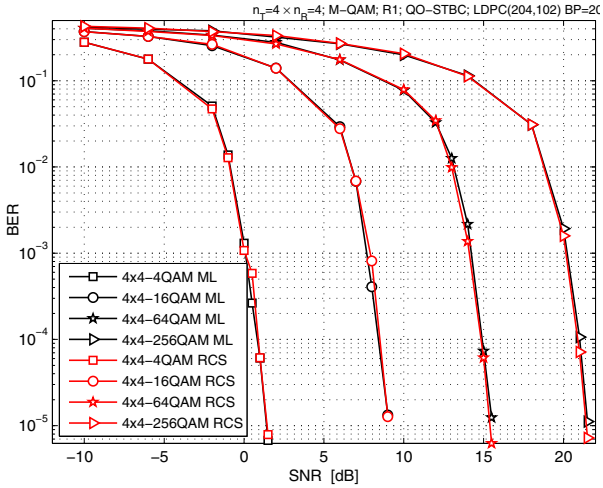

Figure 7. ML against RCS-ML decoding performance comparison for the QO-STBC MIMO system with short LDPC(204,102) and $n_T = 4 \times n_R = 4$ antennas.

Table II
NUMBER OF REAL MULTIPLICATIONS/SUMS PER RECEIVE ANTENNA PER SYMBOL PAIR NECESSARY FOR QO-STBC DECODING, $n_T = 4 \times n_R = 1$.

Decoder	4-QAM	16-QAM	64-QAM	256-QAM
RCS-ML	720/216	2880/864	11520/3456	46080/13824
ML	1440/432	23040/6912	368640/110592	5898240/1769472
CR_{RCS}	50%	12.5%	3.125%	0.781%

order increases, indicating that the RCS-ML becomes an attractive option when $M > 16$.

VI. CONCLUSIONS

In this work, a reduced complexity ML decoding scheme based on cluster search, suitable for QO-STBC coded MIMO systems with higher-order modulation indexes, has been proposed.

Numerical results for the RCS-ML have indicated no degradation in the performance in all analyzed cases. Thanks to reduced cluster search procedure, the RCS-ML achieves the ML performance with an increasing reduction in the computational complexity when the modulation order increases, being 12.5% of ML decoding complexity for 16-QAM, and $< 1\%$ for 256-QAM.

REFERENCES

[1] S. Alamouti, "A simple transmit diversity technique for wireless communications," *IEEE Journal on Selected Areas in Communications*, vol. 16, no. 8, pp. 1451–1458, October 1998.

[2] H. Jafarkhani, *Space-Time Coding: Theory and Practice*. Cambridge University Press, 2005.

[3] N. S. J. Pau, D. P. Taylor, and P. A. Martin, "Robust high throughput space time block codes using parallel interference cancellation," *IEEE Transactions on Wireless Communications*, vol. 7, no. 5, pp. 1603–1613, May 2008.

[4] E. Biglieri, Y. Hong, and E. Viterbo, "On fast-decodable space-time block codes," in *IEEE International Zurich Seminar on Communications*, March 2008, pp. 116–119.

[5] C. Jiang, H. Zhang, D. Yuan, and H.-H. Chen, "A low complexity decoding scheme for quasi-orthogonal space-time block coding," in *SAM 2008 – 5th IEEE Sensor Array and Multichannel Signal Processing Workshop*, July 2008, pp. 9–12.

[6] J. Kim and K. Cheun, "An efficient decoding algorithm for qo-stbcs based on iterative interference cancellation," *IEEE Communications Letters*, vol. 12, no. 4, pp. 292–294, April 2008.

[7] S. Sezginer and H. Sari, "Full-rate full-diversity 2 x 2 space-time codes of reduced decoder complexity," *IEEE Communications Letters*, vol. 11, no. 12, pp. 973–975, December 2007.

[8] D. Choi, C. Chae, and T. Jung, "Design of new minimum decoding complexity quasi-orthogonal space-time block code for 8 transmit antennas," in *IEEE International Symposium on Signal Processing and Information Technology*, Dec. 2007, pp. 674–677.

[9] C. Yuen, Y. L. Guan, and T. T. Tjhung;, "Quasi-orthogonal stbc with minimum decoding complexity: further results," in *IEEE Wireless Communications and Networking Conference*, vol. 1, March 2005, pp. 483–488.

[10] R. Gallager, "Low density parity check codes," *IEEE Transactions on Information Theory*, vol. 8, no. 1, pp. 21–28, January 1962.

[11] D. Mackay and R. M. Neal, "Near shannon limit performance of low density parity check codes," *Electronic Letters*, vol. 33, no. 6, pp. 457–458, March 1997.

[12] D. Mackay, "Good error-correcting codes based on very sparse matrices," *IEEE Transactions on Information Theory*, vol. 45, no. 2, pp. 399–431, March 1999.

[13] H. Jafarkhani, "A quasi-orthogonal space-time block code," *IEEE Transactions on Communications*, vol. 49, no. 1, pp. 1–4, Jan. 2001.

[14] G. Lechner, "Efficient decoding techniques for ldpc codes," Master's thesis, Vienna University of Technology, July 2007.

[15] D. J. MacKay, "Encyclopedia of sparse graph codes," Available at: http://www.inference.phy.cam.ac.uk/mackay, 2003.